A Novel LSO-PI Open-Left UPQC for Dual Load Harmonic Mitigation and Voltage Correction

Y. Priyanka*‡, A. Raghu Ram**

*Department of Electrical and Electronics Engineering, G. Narayanamma Institute of Technology and Science, Shaikpet, Hyderabad, India

**Department of Electrical and Electronics Engineering, Jawaharlal Nehru Technological University College of Engineering, Hyderabad, India

(priya.yerpula@gmail.com, raghuram_a@yahoo.co.in)

‡Corresponding Author: Priyanka Y, G. Narayanamma Institute of Technology and Science, Shaikpet, Hyderabad, India, 500008 Tel:9866190499, priya.yerpula@gmail.com

Received: 16.11.2023 Accepted:14.01.2024

Abstract- This study presents the Leopard seal optimization (LSO)-Proportional Integral (PI) based Open Left Unified Power Quality Conditioner (OL-UPQC), a novel configuration that combines the design structure of open UPQC and left shunt UPQC. This unique design of OL-UPQC mandates the usage of closed loop control systems that rely largely on the operation and performance of the PI controller for both shunt and series converter control. The left shunt converter is designed to suppress harmonics from numerous load sites, therefore it is controlled using the unit vector template (UVT) method, which is strongly reliant on the performance of the PI controller. In an open system, the series converter's independent DC-link voltage control underlines the critical role it plays in ensuring correct performance for voltage-sensitive loads on the left. Thus, its control is based on the synchronous reference frame (SRF) approach, which employs an LSO tuned PI controller for precise control and operation of voltage across sensitive loads. A comprehensive comparison simulation analysis is carried out to assess the efficacy of the proposed configuration. This study demonstrates how the configuration can reduce harmonic pollution from many loads. Furthermore, the configuration's ability to provide voltage compensation in various voltage disturbance scenarios is studied.

Keywords Harmonics; unified power quality conditioner, voltage disturbance, synchronous reference frame, unit vector template.

Nomenclature

LC	load connection points
OL-UPQC	Open-Loop Unified Power Quality Conditioner
PI	Proportional-Integral
PLL	phase locked loop
PQ	Power Quality
SRF	Synchronous Reference Frame
THD	Total Harmonic Distortion
UPQC	Unified Power Quality Conditioner
UVT	Unit vector template

1. Introduction

The current study is increasingly concentrated on comprehensive solutions aimed at mitigating power quality degradation, in response to the observed variations in voltage and current patterns in distribution systems. Voltage fluctuations pose a significant risk to delicate equipment, including advanced medical devices in healthcare facilities, security systems in commercial structures, and the uninterrupted operation of industrial machinery. Moreover, the proliferation of nonlinear loads has led to a substantial rise in the harmonic components seen in source currents over the past few decades. Nonlinear characteristics have the potential to induce distortions in line currents when applied to commonly utilised loads, including computers, switched-mode power supply, various switching components, and

motor drive applications that depend on front-end rectifiers. The Unified Power Quality Conditioner (UPQC) has been identified as the most effective solution for addressing power quality issues in this particular context [1]-[4]. The device possesses several functionalities, such as mitigating harmonic distortion in current and voltage, rectifying voltage, correcting supply voltage and load imbalances, and managing increased reactive power requirements caused by specific loads.

Power Quality (PQ) at the distribution level requires maintaining a power distribution bus voltage that nearly resembles a sinusoidal waveform, keeping its required magnitude and frequency while assuring uninterrupted energy delivery to clients. PQ is divided into two basic components: voltage quality and supply dependability [1]. Voltage quality includes a wide range of disturbances such as fast fluctuations, harmonics, inter-harmonics, flicker, imbalance, and transients. Supply reliability, on the other hand, refers to longer-lasting occurrences such as power outages, voltage dips and sags, over-voltage, under-voltage, and frequency changes. These aspects, taken together, shed light on the underlying reasons of PQ difficulties. Harmonic distortion, a well-known occurrence in power systems, is also a major source of worry.

Among the several UPQC topologies available, UPQC-R [2], [5]-[8] is the most widely used configuration in research projects. The shunt converter is strategically located on the right side of the UPQC, while the series converter is located on the left. This positioning is carefully chosen to avoid the load current passing via injection transformers. The alternate UPQC-L arrangement, in which the shunt converter is on the left and the series converter is on the right, is reserved for specialist applications [9]. According to [10], UPQC-L covers the use of UPQC for specific voltage-sensitive load points as well as the adjustment of current harmonics for numerous load points. It is crucial to note, however, that the actions of these converters are not independent of one another because they are linked by a shared DC-link. As a result, there is a greater chance that both converters will have an influence on each other's performance, which is extremely undesirable in order to avoid degradation in their respective performances. It is ideal to keep the shunt converter, which is in charge of handling harmonic adjustment for various load points, separate from the series converter. Furthermore, because the series converter is in charge of managing voltage-sensitive loads that demand quick reaction due to voltage perturbations that last only a few cycles, having an independent series converter is clearly the preferable choice in such cases.

In recent years, many new alternate arrangements of UPQC have been explored and tested based on their specific applications and requirements. A MO-UPQC has been proposed to handle power quality issues along with real power injection [12]. Likewise, SMES based UPQC has been explored in [13] applicable to DFIG/DC-microgrid hybrid power system. In [14] an UPQC arrangement is proposed for single-phase systems based on two three-leg AC-DC-AC converters. Henceforth, various such altered configurations of UPQC have been found in the research domain. Another such configuration of UPQC is open-UPQC. The Open UPQC illustrated in [15] for comparative analysis with conventional UPQC uses an eternal active source fed series inverter for voltage compensation instead of a passive device like DC-link capacitor. An open-UPQC arrangement can also be adopted as a tool for interaction with the main grid [17] and applicable in smart grid [18]. However, the above stated researches have not primarily focused on power quality improvement attributes. Few other applications of this open-UPQC were observed in power system [19]-[20].

This arrangement of open-UPQC, which uses uncoupled converters, has proved the ability to attain performance characteristics comparable to typical UPQC installations. Open UPQC's fundamental benefit is its ability to stabilize load voltage while also assuring sinusoidal supply current and load voltage, all while preserving balance. End-users in the field benefit greatly from the flexibility inherent in the Open UPQC architecture. It enables the separation of series and shunt converters as needed, allowing for customised responses to individual end-user load profiles.

Control methods, such as Unit vector template (UVT) and Synchronous Reference Frame (SRF) approach, rely largely on accurate tuning and successful functioning of its error processing controller in the area of controlling converters [23]-[25]. Years of experience have continuously shown that the Proportional-Integral (PI) controller is the most robust and pragmatically feasible alternative, particularly for custom power devices such as UPQC control design [26], [27]. Simulation of UPQC for enhancing Power Quality[28].

As a result, when improving a system's control structure to achieve higher flexibility and dynamic responsiveness becomes a main design goal, correct tuning of these PI controller settings to support quick responses becomes critical. Because of its ability to solve sophisticated, high-dimensional, and non-convex optimization difficulties, metaheuristic optimization is critical in the UVT and SRF control technique for current and voltage quality management.

This paper introduces the LSO (Leopard seal optimization)-PI based OL-UPQC (LSO tuned PI based Open Left UPQC) that was customized using the LSO approach. This type of system is useful in rectifier and converter motor drive systems, as well as other load scenarios defined by the presence of harmonics due to switching devices. OL-UPQC, a unique hybrid configuration that combines UPQC-L with open UPQC incorporating LSO tuned PI based control methods for shunt and series converter. It leverages the benefits of open UPQC while effortlessly harmonizing with the needs of UPQC-L applications. Furthermore, both UVT and SRF methods, that are controllers for shunt and series converter respectively, involve PI controller, out of which, in UVT method PI controller is directly responsible for generating the reference signal whereas SRF method PI controller is responsible for generating a part of the reference (i.e. loss component of shunt converter). Thus, PI controller optimized tuning is of utmost importance, especially for UVT based controller.

2. Proposed OL-UPQC Configuration

Figure 1 depicts the suggested arrangement, which includes two unique load connection points (LC). One of these serves as a sensitive point subject to voltage changes, while the other is voltage-insensitive but introduces harmonics into the source current. Figure 1 depicts a distribution system configuration with three-phase nonlinear load at LC1 and

LC2. The load at LC2 which serves as the sensitive coupling point. The OL-UPQC arrangement has two autonomous converter systems: one for voltage compensation (the series converter) connected to LC2, and one for current compensation (the shunt converter) attached to LC1. This particular setup is designed to handle harmonic correction for nonlinear loads at numerous load locations while also mitigating voltage disturbances for voltage-sensitive loads without interfering with one another's functions. Also, investigation of the performance of our suggested control design is carried out and compared to other techniques.

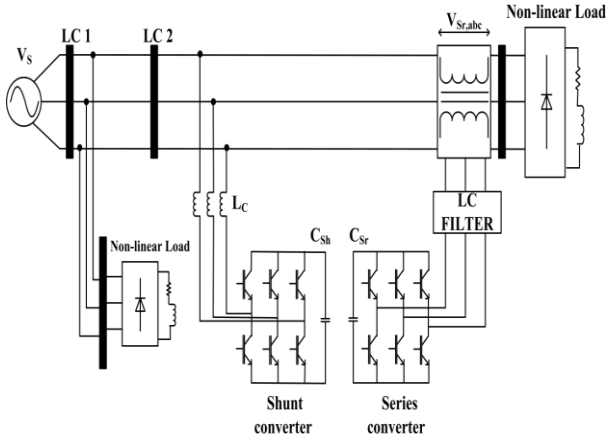


Fig. 1. Proposed configuration of OL-UPQC.

The envisioned configuration of the Open-Loop Unified Power Quality Conditioner (OL-UPQC) comprises two discrete converters operating autonomously without any interconnection. Each converter, whether shunt or series, is configured with three legs tailored for a three-phase three-wire system. Within this design, both converters are equipped with a DC-link capacitor and six IGBT switches. The coupling inductors establish a connection from the shunt section to the distribution system, while the series converter is sequentially integrated into the system via an LC filter. Additionally, a three-phase transformer serves as an injection transformer for the series converter.

The load system encompasses two distinct points of load connections denoted as LC1 and LC2. LC2 is associated with a balanced nonlinear load that exhibits voltage sensitivity, thereby introducing harmonics into the system. Simultaneously, LC1 is linked to a separate three-phase nonlinear load, introducing supplementary harmonics. Consequently, both connected load sites contribute to the introduction of harmonics into the overall system. Notably, the two converters operate independently of one another, ensuring the avoidance of conflicts in their respective tasks.

Control mechanisms differ for the shunt and series converters. The shunt converter is governed by the Unit Vector Template (UVT) control approach [29], while the series converter is subject to control through the Synchronous Reference Frame (SRF) control technique [30], [31]. The pivotal responsibility of the OL-UPQC is to mitigate harmonics emanating from two distinct and independent load sites. Therefore, its control method primarily relies on input from the source current rather than the load current. The decision to employ the UVT control method stems from its exclusive consideration of the source current, omitting the load current from its control framework. The UVT control is intricately linked to the performance of the Proportional-Integral (PI) controller, necessitating a sophisticated optimization process for the fine-tuning of the PI controller.

3. Leopard Seal Optimization (LSO)

The Leopard Seal Optimisation (LSO) algorithm is a bio-inspired optimisation technique that replicates the hunting strategies employed by leopard seals. These highly intelligent organisms demonstrate cooperative behaviour in order to achieve mutual advantages. Leopard seals exhibit a distinct behaviour of actively pursuing and capturing prey, even in the absence of hunger-driven motivations. After a successful act of predation, individuals frequently exhibit a tendency to abstain from immediate intake. The hunting behaviour exhibited by leopard seals can be divided into three distinct phases, namely searching, encircling, and attacking.

(a) Searching of the prey: The ξ position vectors of the ith iteration for the leopard seal Lm can be calculated using (1) [32]

The process of locating the prey involves determining the position vectors, denoted as ξ, for the t^{th} iteration of the leopard seal L_m. This can be achieved by employing equation (1) as described in reference [32].

$$\overrightarrow{Y_\alpha^t}(L_m) = \overrightarrow{D^t}(L_m).\, e^{bf_\alpha} \cos(2\pi f_\alpha) + \overrightarrow{Y_\xi^t}(L_m) \quad (1)$$

The expression $\overrightarrow{Y_\alpha^t}(L_m)$ represents the updated value of α for L_m at the t^{th} iteration. Here, α refers to the position of t^{th} ranging from 2 to ξ-1. The calculation of the distance $\overrightarrow{D^t}(L_m)$ between the leopard seal and its prey can be determined using equation (2), where the logarithmic spiral shape is represented by the variable b. The angle scaling factor, denoted as f_α, is used to determine the position of the leopard seal, specifically its α component. This calculation involves equation (3) and the updated position (denoted as $\overrightarrow{Y_\xi^t}(L_m)$ of the ξ component of L_m at the t^{th} iteration.

$$\overrightarrow{D^t}(L_m) = \left|\overrightarrow{Y_\xi^t}(L_m) - \overrightarrow{Y_1^t}(L_m)\right| \quad (2)$$

$$f_\alpha = 1 - \frac{2\times\alpha}{\xi} \quad (3)$$

The vector $\overrightarrow{Y_1^t}(L_m)$ represents the updated first position of L_m at the t^{th} iteration. α denotes the current location of L_m, whereas ξ represents the total number of positions of L_m.

(b) Encircling the prey: Search agents can wander randomly and non-linearly throughout the search phase to explore the search space. This method explores a wide range of search space areas to find regions with higher

objective function values. These regions suggest prey sites and best solutions. The encircling phase allows search agents to strategically arrange themselves around the prey, the best solution. Equations (4) through (8) can dynamically update leopard seal spatial coordinates during encircling. First, calculate the distance between each search agent and the probable prey to establish its new position. This computation should follow equation (4) [29]. The new search agent's position is calculated next.

$$\overrightarrow{D_{L_m}^t} = \left|\vec{C}\overrightarrow{Y_{prey}^t} - \overrightarrow{Y_{L_m}^t}\right| \quad (4)$$

$$\overrightarrow{Y_{L_m}^{t+1}} = \overrightarrow{Y_{prey}^1} - \vec{A}.\overrightarrow{D_{L_m}^t} \quad (5)$$

$$\vec{A} = 2.\vec{a}.\overrightarrow{r_1} - \vec{a} \quad (6)$$

$$\vec{C} = 2.\overrightarrow{r_2} \quad (7)$$

$$\vec{a} = 2 - t \times \frac{2}{N_{ENC}} \quad (8)$$

The projected location of the prey at a given iteration is denoted as $\overrightarrow{Y_{prey}^t}$, whereas $\overrightarrow{Y_{L_m}^t}$ represents the position of the m^{th} leopard seal at the same iteration. Additionally, $\overrightarrow{D_{L_m}^t}$ refers to the distance between the m^{th} search agent and the prey. Additionally, the vectors $\overrightarrow{r_1}$ and $\overrightarrow{r_2}$ are randomly generated vectors that belong to the interval [0,1]. The coefficient vectors $\vec{A}$ and $\vec{C}$ are computed using equations (6) and (7) with values [29]. The variable NEnc represents the number of iterations in the encircling phase. The vector $\vec{a}$ falls linearly from 2 to 0 throughout the iterations, as calculated using equation (8). In the encircling phase, vector $\vec{A}$ is initialised with a random value selected from the interval [-1, 1].

(c) Attacking the prey: Following the successful completion of the prey encircling process, the subsequent phase commences, known as the attack phase. During this stage, the prey becomes immobilised, rendering it incapable of movement, while the search agents closely approach it. The calculation of the distance between the leopard seal and its possible victim during the attack phase can be determined using equation (9).

$$\overrightarrow{D_{L_m}^{iter}} = \left|\overrightarrow{Y_{prey}^{iter}} - \overrightarrow{Y_{L_m}^{iter}}\right| \quad (9)$$

Where $\overrightarrow{Y_{prey}^t}$ is the predicted location of the prey at the iteration (iter), $Y_{L_m}^{iter}$ is the mth search agent's position at iteration i, $\overrightarrow{D_{L_m}^{iter}}$ is the distance between the mth leopard seal and the potential. The manuscript discusses the fitness function of the proposed strategy, as described in equation (10), which is designed to minimise costs by effectively tuning the proportional gain (k_p) and integral gain (k_i) parameters of the proportional-integral (PI) controller employed in the open-loop unified power quality conditioner (OL-UPQC).

The cost (OF) is a function of the parameters k_p and k_i. The selected cost function for our design is the integral absolute error (ITAE).

$$OF = f(k_p, k_i) \quad (10)$$

Table 1 depicts the algortmic steps for solving the PI controller parameters

Table 1. PSEUDO code of the LSO algorıthm for the present problem

Step 1: Set up the nls leopard seals population as instructed below.

for each $\boldsymbol{L_i} \in \boldsymbol{pack}$**do**

L_i = initialize_greywolf_population() as given below

$$D = \begin{bmatrix} {K_{pt}}^{11}{K_{it}}^{11} & {K_{pt}}^{12}{K_{it}}^{12} & \cdots & {K_{pt}}^{1n}{K_{it}}^{1n} \\ {K_{pt}}^{21}{K_{it}}^{21} & {K_{pt}}^{22}{K_{it}}^{22} & \cdots & {K_{pt}}^{2n}{K_{it}}^{2n} \\ \vdots & \vdots & \vdots & \vdots \\ {K_{pt}}^{m1}{K_{it}}^{m1} & {K_{pt}}^{m2}{K_{it}}^{m2} & \cdots & {K_{pt}}^{mn}{K_{it}}^{mn} \end{bmatrix}$$

split L_i arbitrarily into autonomous groups

end for

Step 2: Set the exploration rate a to 2 and use equations (6) and (7), respectively, to find the coefficients of A and C.

If (leopard seals agent L_i is within boundary range)

Calculate the fitness value of agent (i.e. minimization of integral absolute error (ITAE)) using (10)

Else

fitness value =infinity

End if

while $(\boldsymbol{iter} \leq \boldsymbol{iter^{max}})$ ***do***

for each $\boldsymbol{L_i} \in \boldsymbol{pack}$**do**

Revise the existing agent of the leopard seals based on equation (5).

end for

Linearly decrease the value of variable 'a' from 2 to 0 throughout each iteration using equation (8). Update variables 'A' and 'C' according to equations (6) and (7) correspondingly.

if updated grey wolf agent L_i is within boundary range then

Calculate the fitness value of agent (i.e. minimization of integral absolute error (ITAE)) using (10)

else

fitness of position=infinity

end if

Revise the existing agent of the leopard seals based on equation (5).

iter=iter+1

end while

Choose the most suitable leopard seals agent.

4. LSO Tuned PI based SRF Control for Open-Left Unified Power Quality Conditioner Configuration

4.1 LSO tuned PI based UVT (Unit Vector Template) based Control for Shunt Converter

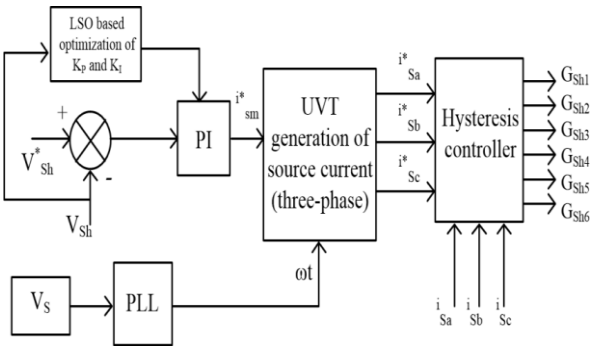


Fig. 2. LSO tuned PI based UVT control for shunt converter.

The regulation of the shunt converter section within the Open-Loop Unified Power Quality Conditioner (OL-UPQC) employs the Unit Vector Template (UVT) approach, a choice made after careful consideration of alternative methods such as Synchronous Reference Frame (SRF) or Active-Reactive Power (PQ) control techniques. The preference for the UVT technique is grounded in its demonstrated suitability for this specific design, distinguishing it from other control methodologies.

The distinctive feature of the UVT approach lies in its independence from load current feedback, setting it apart from other control methods. Instead, the UVT method places the onus of harmonics reduction on two critical factors: the precise control of the DC-link voltage across the shunt capacitor and the current from the power supply source. Consequently, achieving precise and rapid control of the DC-link voltage becomes paramount, contingent upon the performance and responsiveness of the Proportional-Integral (PI) controller.

Illustrated in Figure 2, the control technique involves a continuous comparison of the actual DC-link voltage across the shunt capacitor with its predetermined reference value. Any deviation from this reference value serves as input to the PI controller. The fine-tuning of PI parameters is achieved through the application of the heLC of LSO optimization method. The PI controller processes the current error and generates an output that becomes the basis for determining the maximum source current, thus establishing a robust foundation for effective harmonics reduction within the OL-UPQC system.

$$i^*_{sm} = (V^*_{DC1} - V_{DC1})(K_P + \frac{K_I}{s}) \quad (11)$$

This peak source current value is then utilized in the creation of three reference source current signals.

$$i^*_{sa} = i^*_{sm} \sin \omega t \quad (12)$$

$$i^*_{sb} = i^*_{sm} \sin(\omega t - 120) \quad (13)$$

$$i^*_{sc} = i^*_{sm} \sin(\omega t - 240) \quad (14)$$

These reference source currents are then juxtaposed with the actual respective three-phase source current in a hysteresis controller. In hysteresis controller each phase reference currents are compared with their sensed counterparts and are regulated in a hysteresis band with a tolerance limit of ±1.5 % to generate the shunt converter's basic switching pattern (G_{sh1} to G_{sh6}).

4.2. LSO Tuned PI based SRF Control for Series Converter

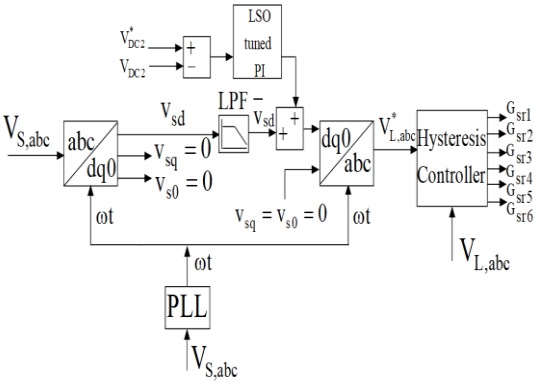


Fig. 3. LSO tuned PI based SRF control for series converter.

Fig. 3 depicts the control approach for the series converter section, which is based on the Synchronous Reference Frame (SRF) algorithm. Given that the series converter is coupled to a DC-link capacitor rather than an external DC source, it is critical to account for DC-link voltage error in the control mechanism to provide rapid transient response, as shown in [15]. The SRF approach, with its control structure, allows for the incorporation of this element, which distinguishes it from the UVT method [15]. The abc-dq transformation is used to convert the three-phase source voltage to two-phase, followed by filtering to reduce harmonics.

The three phase load voltages are changed into the resulting d axis load voltage using the abc to dq transformation as:

$$\begin{bmatrix} v_{l0} \\ v_{ld} \\ v_{lq} \end{bmatrix} = \sqrt{\frac{2}{3}} \begin{bmatrix} \frac{1}{\sqrt{2}} & \frac{1}{\sqrt{2}} & \frac{1}{\sqrt{2}} \\ \sin\theta & \sin\left(\theta - \frac{2\pi}{3}\right) & \sin\left(\theta + \frac{2\pi}{3}\right) \\ \cos\theta & \cos\left(\theta - \frac{2\pi}{3}\right) & \cos\left(\theta + \frac{2\pi}{3}\right) \end{bmatrix} \begin{bmatrix} v_{la} \\ v_{lb} \\ v_{lc} \end{bmatrix} \quad (15)$$

ωt is the transformation angle received from the phase locked loop (PLL) block

The filtered d axis magnitude is combined with the processed error from LSO tuned PI controller that accounts for the loss component of series converter. This resultant is changed from two-phase to three-phase using the dq to abc transformation, coupled with null values for q and zero axis quantity. Thus, applying the dq-abc transformation, the three reference load voltages are produced as follows:

$$\begin{bmatrix} v^*_{La} \\ v^*_{Lb} \\ v^*_{Lc} \end{bmatrix} = \begin{bmatrix} \cos\omega t & -\sin\omega t & 1 \\ \cos\left(\omega t - \frac{2\pi}{3}\right) & -\sin\left(\omega t - \frac{2\pi}{3}\right) & 1 \\ \cos\left(\omega t + \frac{2\pi}{3}\right) & -\sin\left(\omega t + \frac{2\pi}{3}\right) & 1 \end{bmatrix} \begin{bmatrix} \bar{v}_{sd} \\ 0 \\ 0 \end{bmatrix} \quad (16)$$

The resulting three-phase reference load voltage is compared to the actual load voltage in a hysteresis controller to create switching signals for the series converter.

5. Outcome and Discussion

An extensive simulation study is conducted to assess the performance of the proposed LSO-tuned Proportional-Integral (PI) based Open-Loop Unified Power Quality Conditioner

(OL-UPQC) system under diverse scenarios. The simulation involves the introduction of a three-phase nonlinear load at LC1, and a similar three-phase nonlinear load is modeled at LC2. The shunt converter component of the OL-UPQC system undergoes rigorous testing to gauge its effectiveness in compensating for harmonics, while the series converter section is scrutinized for its proficiency in voltage compensation. Moreover, a comprehensive comparative analysis is undertaken to underscore the superior efficacy resulting from the LSO-based optimization of PI controllers for both the shunt and series converters.

The simulation parameters governing this study are meticulously detailed in Table 2, providing a comprehensive overview of the conditions and variables employed to examine the OL-UPQC system under various scenarios. This multifaceted simulation aims to comprehensively evaluate the system's response and performance in the presence of nonlinear loads, shedding light on the nuanced capabilities of both the shunt and series converter components when subjected to LSO-tuned PI controllers.

Table 2. System parameters for simulation

Source Voltage	Internal Impedance	R = 0.1 Ω, L = 0.25 mH
	Voltage (L-L)	395 V
	Line frequency	50 Hz
Shunt converter	Coupling Inductor	2.25 mH
Series converter	L, C Filter	2.6 mH, 62 µF
	Transformer	100:100, 3.0 kVA
DC capacitor	Capacitance	C_{DC1}=2400 µF and C_{DC2}=2400 µF
	Reference Voltage	715 V
LC1 Load	3 Ø nonlinear load	R = 27 Ω, L = 8 mH
LC2 Load	3 Ø nonlinear load	R = 30 Ω, L = 12 mH

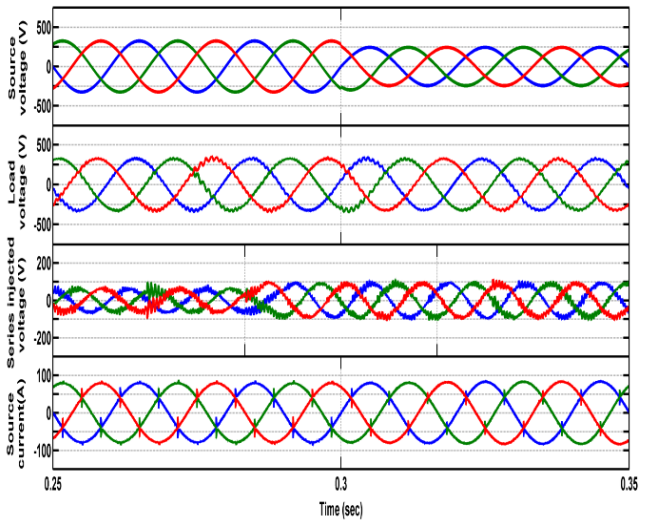


Fig. 4(a). Voltage sag condition: supply voltage (V), load voltage (V), series injected voltage (V), source current (A) [top to bottom].

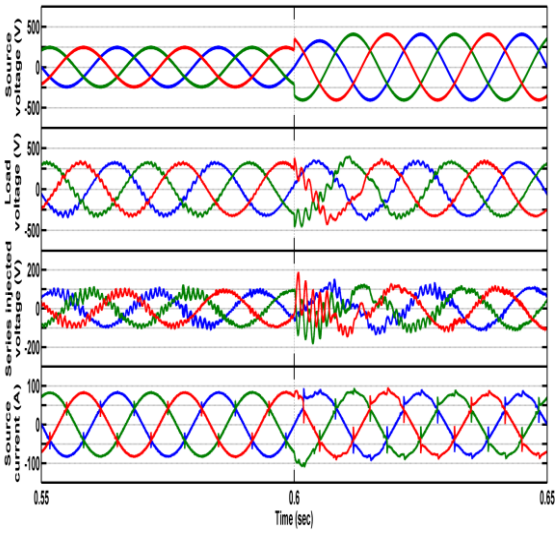


Fig. 4(b). Voltage swell condition: supply voltage (V), load voltage (V), series injected voltage (V), source current (A) [top to bottom].

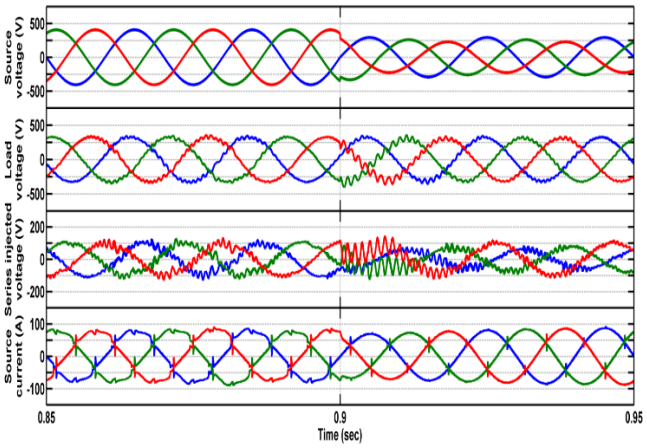


Fig. 4(c). Voltage unbalance condition: supply voltage (V), load voltage (V), series injected voltage (V) [top to bottom].

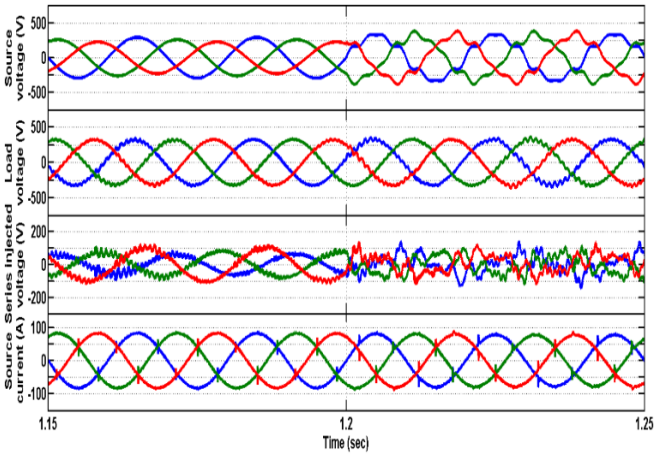


Fig. 4(d). Voltage harmonic condition: supply voltage (V), load voltage (V), series injected voltage (V) [top to bottom].

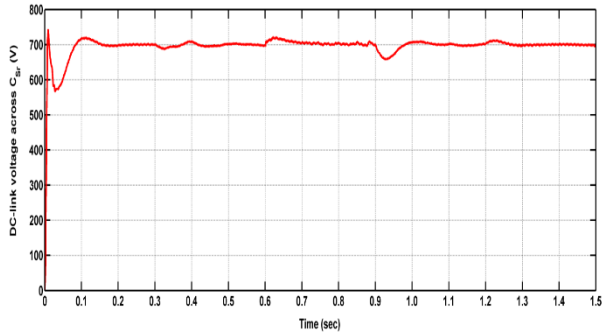


Fig. 4(e). Voltage across DC-link capacitor C_{Sr}.

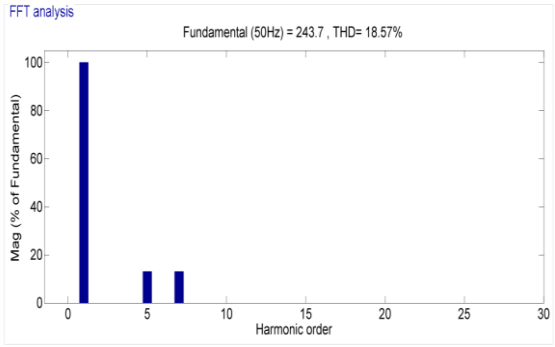


Fig. 4(f). THD spectrum analysis of load voltage without compensation.

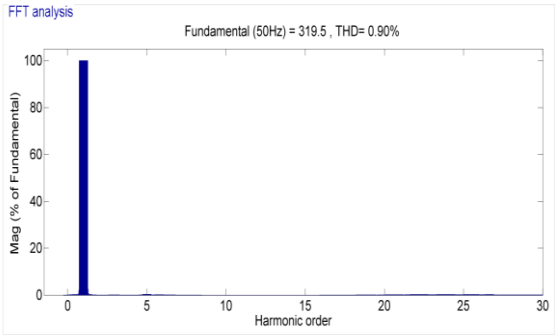


Fig. 5(g). THD spectrum analysis of load voltage after compensation.

5.1. Voltage Disturbance Condition

Performance analysis of OL-UPQC initiates with voltage disturbance in the form of supply voltage sag, thus analyzing the response from series converter of OL-UPQC. A voltage sag of 25 % is introduced at 0.25 s. Fig. 4(a) illustrates the response of series converter under sag condition. With quick response from series converter, the load voltage is compensated and is maintained at the set reference value irrespective of the sag in the supply. Also, the appropriate series injected voltage is shown in the same figure. Fig. 4(b) indicates the simulation waveform under voltage swell condition. A voltage swell of 25 % is introduced with the source voltage at 0.6 s in the waveform depicted between 0.55 s to 0.65 s. With an effective series injection of voltage from series converter, the load voltage is maintained at the set reference value, shown in the same figure. Fig. 4(c) indicates the voltage unbalance condition in terms of magnitude of three phases. As shown, with proper compensation from series converter the load voltage is again set back to its reference value. Moreover, voltage harmonic compensation ability of series converter is depicted with Fig. 4(d). As shown in the figure, source voltage is contaminated with harmonics which will also appear across the voltage sensitive load at LC2. With appropriate and quick response from series converter, the load voltage is free from harmonics as observed from the results. The voltage across DC-link capacitor of series converter is maintained at its set reference value irrespective of voltage disturbance as shown in Fig. 4(e). Also, on performing THD (total harmonic distortion) analysis on the source voltage, its THD content is found to be around 18 % as shown in Fig. 4(f), but the load voltage after compensation has THD of 0.89 % as shown in Fig. 4(g).

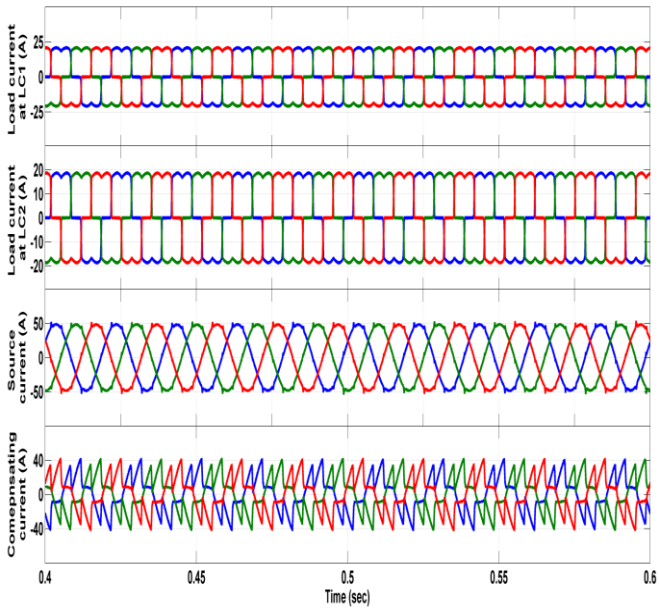


Fig. 5(a). Current harmonic compensation scenario: load current drawn at LC1 (A), load current drawn at LC2 (A), source current drawn from supply (A), compensating current injected from shunt converter (A).

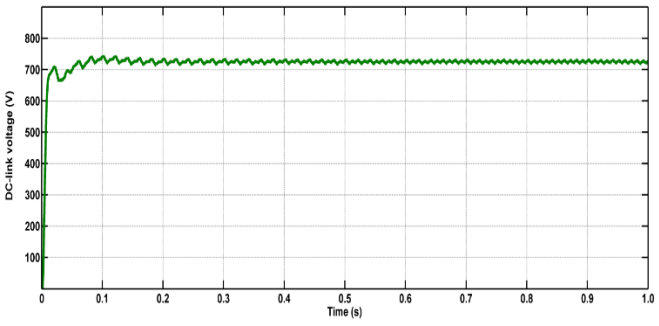


Fig. 5(b). Voltage across DC-link capacitor C_{Sh}.

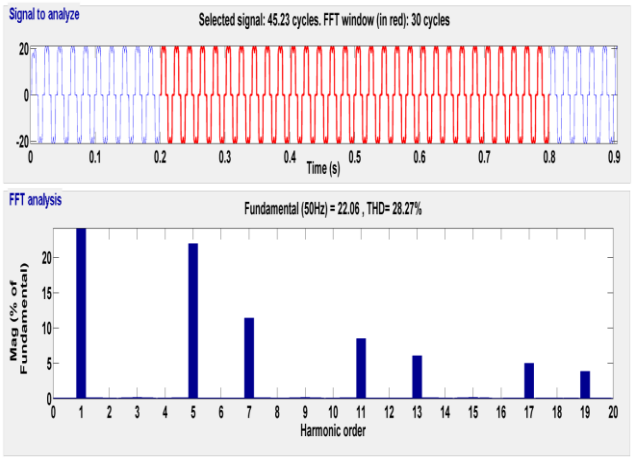


Fig. 5(c). THD spectrum analysis of load current at LC1

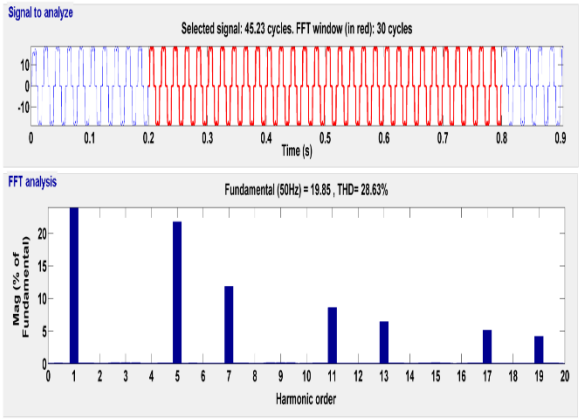


Fig. 5(d). THD spectrum analysis of load current at LC2

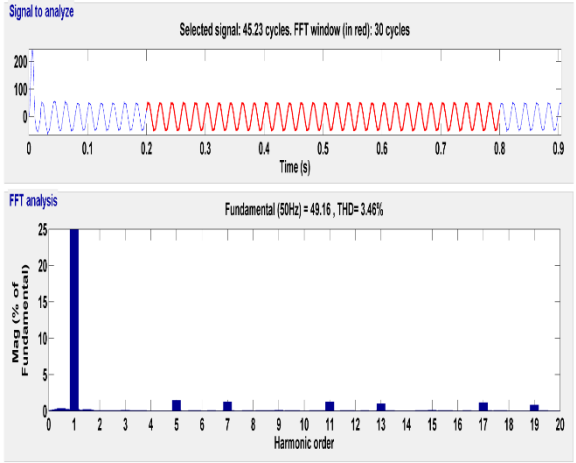


Fig. 5(e). THD spectrum analysis of source current

5.2. Current Harmonics Condition

The evaluation of the shunt converter segment within the OL-UPQC system focuses on its efficacy in mitigating harmonics introduced into the source current by non-linear loads at both LC1 and LC2 connection points. In Figure 5(a), multiple current waveforms, including the load current at LC1, the load current at LC2, the power supply source current, and the compensatory current supplied by the shunt converter, are illustrated. Noteworthy findings emerge from this depiction.

Both load currents exhibit significant deviations from a sinusoidal waveform pattern. However, following correction by the OL-UPQC's shunt converter component, the source current becomes balanced and approaches a nearly sinusoidal waveform. The pattern of the compensating current is also evident, highlighting its efficiency in suppressing harmonics.

Furthermore, Figure 5(b) illustrates the consistent maintenance of the voltage across the shunt converter's DC-link capacitor at its predetermined reference value. A total harmonic distortion (THD) analysis of the load currents at LC1 and LC2 is presented in Figure 5(c) and Figure 5(d), revealing reasonably high THD values of 28.27% and 28.63%, respectively. The presence of harmonics is accountable for these elevated THD levels. In Figure 5(e), the THD spectrum analysis of the source current post-correction indicates a significant reduction in THD to 3.46%. This post-compensation THD value falls within IEEE standard limits, providing clear evidence that the OL-UPQC's shunt converter component successfully mitigates harmonics, demonstrating its effectiveness in improving the quality of the source current.

5.3. PI Controller Tuning Comparative Investigation

The behavior of the DC-link capacitor voltage stands as a critical determinant of the overall system's performance, particularly in its response to transient events such as initial states or changes in load conditions within UPQC power conditioning systems. Within this framework, we leverage the DC-link voltage profile as a pivotal analytical indicator to assess the effectiveness of the proposed LSO-tuned PI-based approach in the context of the OL-UPQC system. Several alternative optimization strategies, including Grey Wolf Optimization (GWO), Red Piranha Optimization (RPO), White Shark Optimization (WSO), and Genetic Algorithm (GA), are considered for the fine-tuning of the PI controller.

Figure 6 provides a visual representation of the DC-link voltage patterns generated by these diverse optimization approaches over a 5-second time span within an 800 V voltage range. At the 1.0-second mark, an additional nonlinear load is introduced at LC1 to scrutinize the system's transient reactions. Parameters such as initial reaction time, transient response time, and variations observed during transient circumstances are integral components of this comprehensive investigation. The outcomes are tabulated in Table 3, presenting a comparative analysis.

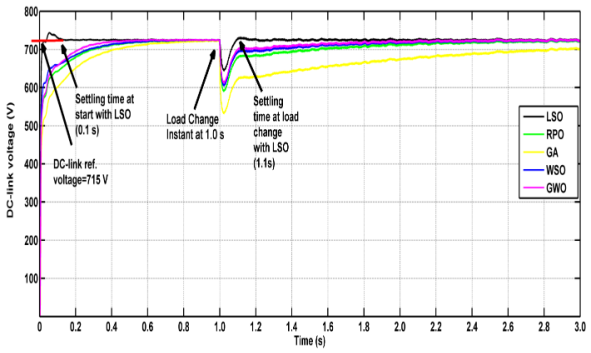


Fig. 6. DC-link voltage comparison utilizing several optimization methods.

The results and data unequivocally demonstrate the superior performance of the proposed LSO-tuned strategy compared to previous optimization methodologies. Notably, the pattern of the DC-link voltage profile exerts a significant influence on the performance characteristics of the OL-UPQC system. In contrast to the GWO optimization and surpassing other methodologies, the LSO method yields exceptional results, showcasing approximately 76% and 83% reductions in reaction times during the initial phase (starting) and transient situations (load variations), respectively. This underscores the efficacy and superiority of the LSO-tuned PI-based approach in enhancing the performance of the OL-UPQC system under varying conditions.

Furthermore, the LSO method's compensation performance is outstanding, resulting in a source current THD of 3.46% under the same load circumstances. This figure is lower than the other approaches, which have greater THD values. The data given clearly demonstrates the efficacy of the suggested strategy in terms of harmonic mitigation and response time.

Table 3. Different optimization of PI tuning comparative investigation

PI optimization technique	PI parameter values (K_P and K_I)	Settling-time during start (s)	Dip in voltage at start (%)	Settling-time during load change (s)	THD of source current (%)
LSO	0.17, 6.8	0.1	4.8	0.1	3.46
GWO	1.7, 11.8	0.55	9.6	1.2	4.78
WSO	3.2, 14.5	0.75	10.1	1.6	5.35
RPO	4.3, 17.9	0.85	13.1	1.8	6.68
GA	7.2, 19.4	0.95	21.3	4.9	6.74

6. Conclusion

The proposed system employs a unique dual-load-point setup, implementing an Open Unified Power Quality Conditioner (OL-UPQC) system with uncoupled shunt and series converters. The control mechanisms are based on LSO-tuned Proportional-Integral (PI) controllers, distinguishing it as a pioneering approach. Notably, the shunt converter is strategically positioned on the left side of the overall system, while the series converter occupies the right side. This distinctive configuration has proven highly effective in addressing harmonic distortions originating from various individual load locations and managing voltage-sensitive loads. The OL-UPQC system serves a dual purpose: firstly, mitigating harmonic distortions generated by nonlinear loads connected to LC1 and LC2, and secondly, ensuring voltage stability for sensitive loads linked to LC2. The shunt and series converters operate under the Unit Vector Template (UVT) and Synchronous Reference Frame (SRF) control methods, respectively, both supported by LSO-tuned PI controllers. Simulation tests demonstrate the commendable performance of the OL-UPQC system in both steady-state and transient conditions. The system exhibits rapid and dynamic responses, effectively managing Total Harmonic Distortion (THD) in the source current, maintaining it at approximately 3.46% to comply with set limitations. The OL-UPQC reliably balances and sustains load voltage at the required reference level, even during transient occurrences and various voltage-related disturbances such as sag, swell, unbalancing, and harmonics. A comparative analysis highlights the superior efficiency of the proposed LSO-tuned PI controller in contrast to other optimization methods. This underscores the robustness and effectiveness of the LSO-tuned PI-based OL-UPQC system.

As part of future research prospectives observed from the investigation carried out in the manuscript can be listed as: 1. Investigate the adaptability and performance of the OL-UPQC system in more complex power distribution systems with multiple interconnected nodes. 2. Explore the integration of renewable energy sources within the OL-UPQC framework to assess its applicability and performance in modern, sustainable power systems. 3. Investigate the system's response to dynamic load variations and explore strategies for enhancing its adaptability to changing load profiles. 4. Examine practical implementation challenges and scalability issues to facilitate the seamless integration of the OL-UPQC system into existing power infrastructures.

References

[1] M. Srivastava, S. K. Goyal, A. Saraswat, R. S. Shekhawat and G. Gangil, “A review on power quality problems, causes and mitigation techniques”, 2022 1st International Conference on Sustainable Technology for Power and Energy Systems (STPES), SRINAGAR, India, 2022, pp. 1-6.

[2] V. Khadkikar, “Enhancing electric power quality using UPQC: A comprehensive overview”, IEEE Trans. Power Electronics, Vol. 27, No. 5, pp. 2284 - 2297, May 2012.

[3] S. S. Bhosale, Y. N. Bhosale, U. M. Chavan and S. A. Malvekar, “Power quality improvement by using UPQC: A review”, 2018 International Conference on Control, Power, Communication and Computing Technologies (ICCPCCT), Kannur, India, 2018, pp. 375-380.

[4] A. Heenkenda, A. Elsanabary, M. Seyedmahmoudian, S. Mekhilef, A. Stojcevski and N. F. A. Aziz, “Unified power quality conditioners based different structural arrangements: A comprehensive review”, in IEEE Access, vol. 11, pp. 43435-43457, 2023.

[5] V. M. C. Moreira, J. A. P. Lopes, C. H. Antunes, G. J. Osório, J. P. S. Catalão, J. L. Afonso, “A novel three-phase multiobjective unified power quality conditioner”, in IEEE Transactions on Industrial Electronics, vol. 71, no. 1, pp. 59-70, Jan. 2024.

[6] Shandilya and R. Singh, “Fuzzy controller based solar connected UPQC to enhance power quality in distribution system”, 2023 IEEE Renewable Energy and Sustainable E-Mobility Conference (RESEM), Bhopal, India, 2023, pp. 1-6.

[7] J. T. Cardoso, C. B. Jacobina, P. L. S. Rodrigues and A. M. N. Lima, “PUC converter based on AC-DC-AC multilevel topologies with a shared leg”, in IEEE Transactions on Industry Applications, doi: 10.1109/TIA.2023.3292817.

[8] X. Zhu, Y. Guo, S. Li, J. Deng, T. Ji, “Optimal location and capacity planning of UPQCs considering operation dispatching in distribution grid with distributed generators”, Energy Reports, vol. 8, no. 13, 2022, pp. 832-842.

[9] Ghosh, A., Jindal, A., K., and Joshi, A., "A unified power quality conditioner for voltage regulation of critical load bus", IEEE Power Eng. Soc. Gen. Meet., pp. 471–476, June 2004.

[10] Nishant Patnaik & Anup Kumar Panda, "Extensive application of UPQC-L for a dual point of common coupling system with multiple loads under unbalanced source condition", Electric Power Components and Systems, vol. 45, no.15, pp. 1653-1666, 2017.

[11] R. Zhang, L. Wang, X. Hu, W. Zhou, S. Yang, Z. Li, Z. Cheng, C. Su "A dual control for DFIG/DC-microgrid hybrid power system employing smes-based unified power quality conditioner", 2023 IEEE International Conference on Applied Superconductivity and Electromagnetic Devices (ASEMD), Tianjin, China, 2023, pp. 1-2.

[12] G. F. Da Paz, C. B. Jacobina, I. S. de Freitas, J. T. Cardoso and A. d. Q. T. B. Mesquita, "Unified power quality conditioner (UPQC) based on two three-leg converters with standby operation mode and improved voltage swell compensation", 2023 IEEE Energy Conversion Congress and Exposition (ECCE), Nashville, TN, USA, 2023, pp. 1318-1325.

[13] M. Brenna, R. Faranda and E. Tironi, "A new proposal for power quality and custom power improvement: OPEN UPQC", in IEEE Transactions on Power Delivery, vol. 24, no. 4, pp. 2107-2116, Oct. 2009.

[14] J. Kotturu and P. Agarwal, "Comparative performance analysis of UPQC and open UPQC", 2015 Annual IEEE India Conference (INDICON), New Delhi, India, 2015, pp. 1-6.

[15] M. C. Falvo, M. Manganelli, R. Faranda and H. Hafezi, "Smart n-grid energy management with an open UPQC", 2016 IEEE 16th International Conference on Environment and Electrical Engineering (EEEIC), Florence, Italy, 2016, pp. 1-6.

[16] H. Hafezi and R. Faranda, "Open UPQC series and shunt units cooperation within Smart LV Grid", 2017 6th International Conference on Clean Electrical Power (ICCEP), Santa Margherita Ligure, Italy, 2017, pp. 304-310.

[17] T. Wei and D. Jia, "A new topology of OPEN UPQC", 2014 9th IEEE Conference on Industrial Electronics and Applications, Hangzhou, China, 2014, pp. 1313-1318.

[18] J. Kotturu and P. Agarwal, "Performance analysis of Open UPQC using three level diode clamped multilevel converter", 2016 IEEE 6th International Conference on Power Systems (ICPS), New Delhi, India, 2016, pp. 1-6.

[19] M. A. Amini, A. Jalilian, "Modelling and improvement of open-UPQC performance in voltage sag compensation by contribution of shunt units", Electric Power Systems Research, vol. 187, 2020.

[20] M. Amini, A. Jalilian, "Optimal sizing and location of open-UPQC in distribution networks considering load growth", International Journal of Electrical Power & Energy Systems, vol. 130, 2021.

[21] A. A. Imam, R. S. Kumar, Y. A. Al-Turki, "Modeling and simulation of a PI controlled shunt active power filter for power quality enhancement based on P-Q theory", Electronics, vol. 9, no. 4, p. 637, Apr. 2020.

[22] R. R. Chegudi, B. Ramadoss, A. R. K. Rao, "Artificial rabbits optimization based optimal allocation of solar photovoltaic systems and passive power filters in radial distribution network for power quality improvement", International journal of intelligent engineering and systems, Vol.16, No.1, pp.100-109, 2023.

[23] K. S. Dedy, A. M. Ashari, S. Heri, "Transient operation of a four-leg inverter in rooftop solar connected to a grid using optimized constructive neural network", International journal of intelligent engineering and systems, Vol.14, No.6, pp.258-273, 2021.

[24] A. K. Mishra, P. K. Ray, A. K. Patra, R. K. Mallick, S. R. Das, (2020). Self-tuned PI Controller Based Hybrid Shunt Active Power Filter for Power Quality Enhancement. In: Pradhan, G., Morris, S., Nayak, N. (eds) Advances in Electrical Control and Signal z665. Springer.

[25] H. Ghasemian, F. Ghasemian, and H. Vahdat-Nejad, 2020. Human Urbanization Algorithm: A Novel Metaheuristic Approach. Mathematics and Computers in Simulation, 178, pp.1-15.

[26] Z. Reguieg, I. Bouyakoub, F. Mehedi, F. Bouhadji, "Optimizing power quality: simulation of UPQC integrated PV with comprehensive reliability and performance analysis" International Journal of Smart Grid, vol 8, No1, March 2024.

[27] A. K. Panda & N. Patnaik, "Combined operation of a new power angle control unit vector template based unified power quality conditioner and fuel cell stack supply with effective utilization of shunt and series converter", Electric Power Components and Systems, vol. 44, no. 18, pp.2048-2058, 2016.

[28] N. Patnaik, A. K. Panda, "Performance analysis of a 3 phase 4 wire UPQC system based on PAC based SRF controller with real time digital simulation", International Journal of Electrical Power & Energy Systems, vol. 74, pp. 212-221, 2016.

[29] A. K. Panda, N. Patnaik, "Management of reactive power sharing & power quality improvement with SRF-PAC based UPQC under unbalanced source voltage condition", International Journal of Electrical Power & Energy Systems, vol. 84, pp. 182-194, 2017.

[30] A. H. Rabie, N. A. Mansour, and A. I. Saleh, "Leopard seal optimization (LSO): A Natural Inspired Meta-Heuristic Algorithm. Communications in Nonlinear Science and Numerical Simulation, p.107338, 2023.